Oxidation Resistance of Graphene-Coated Cu and Cu/Ni Alloy

Shanshan Chen,[⊥,‡,†] Lola Brown,[⊥,§] Mark Levendorf,[§] Weiwei Cai,[†,‡] Sang-Yong Ju,[§] Jonathan Edgeworth,[‡] Xuesong Li,[‡] Carl W. Magnuson,[‡] Aruna Velamakanni,[‡] Richard D. Piner,[‡] Junyong Kang,[†] Jiwoong Park,[§,∥,*] and Rodney S. Ruoff[‡,*]

[‡]Department of Mechanical Engineering and Texas Materials Institute, University of Texas at Austin, Austin, Texas 78712, United States , [†]Department of Physics, Xiamen University, Xiamen 361005, China, [§]Department of Chemistry and Chemical Biology, and [∥]Kavli Institute at Cornell for Nanoscale Science, Cornell University, Ithaca, New York 14853, United States. [⊥]These authors contributed equally to this work.

ABSTRACT The ability to protect refined metals from reactive environments is vital to many industrial and academic applications. Current solutions, however, typically introduce several negative effects, including increased thickness and changes in the metal physical properties. In this paper, we demonstrate for the first time the ability of graphene films grown by chemical vapor deposition to protect the surface of the metallic growth substrates of Cu and Cu/Ni alloy from air oxidation. In particular, graphene prevents the formation of any oxide on the protected metal surfaces, thus allowing pure metal surfaces only one atom away from reactive environments. SEM, Raman spectroscopy, and XPS studies show that the metal surface is well protected from oxidation even after heating at 200 °C in air for up to 4 h. Our work further shows that graphene provides effective resistance against hydrogen peroxide. This protection method offers significant advantages and can be used on any metal that catalyzes graphene growth.

KEYWORDS: graphene · oxidation · coating · protection · impermeability · chemical inertness

The use of refined metals is widespread, but they are often chemically reactive, requiring protective coatings for many applications. Protecting the surface of reactive metals has developed into a significant industry which employs many different approaches, including coating with organic layers,[1−3] paints or varnishes,[4] polymers,[5] formation of oxide layers,[6] anodization,[7] chemical modification,[8] and coating with other metals or alloys.[9] However, most conventional methods modify the physical properties of metals being protected. The addition of a protective coating changes the dimensions of the metal due to the finite thickness of the coating, changes the appearance and the optical properties of the metal surface, and often decreases the electrical and thermal conductivity. One important approach to overcome these problems would be to develop an ultrathin protection coating with minimum changes to the physical properties of the protected metal.

Graphene as a two-dimensional one-atom-thick sheet of carbon has attracted increased interest due to both fundamental reasons and its potential for a wide variety of applications.[10−13] A worldwide effort (our group included)[14−18] is underway on developing new and improved methods of growing graphene on metal substrates. In particular, chemical vapor deposition (CVD) techniques have been successfully applied to grow high quality single layer and multilayer graphene onto various metal substrates, including single-layer growth on Cu,[17,19] Pt,[20] and Ir,[21] and multilayer growth on Ni[15,22] and Ru.[23] Growth temperature ranges from 650 to above 1000 °C, depending on the substrate of choice and the carbon source used.[15,17,19−25] In this paper we show that graphene acts as an optically thin oxidation barrier to a pure, unoxidized metal surface. This protection layer maintains a smooth metal surface with many atomic steps,[17] with surface topology significantly different from uncoated metal surfaces. This new kind of surface, where the unoxidized metal is only one atom away from the surface, can open up the way to novel sensing and energy harvesting applications.

The full potential of graphene as a protection layer can be understood based on its unique physical and chemical properties. First, surfaces of sp^2 carbon allotropes form a natural diffusion barrier thus providing a physical separation between the protected metal and reactants. This can be seen from the encapsulation of various atomic species inside of fullerenes and carbon nanotubes at high temperatures and in vacuum.[26] More recently, graphene has been used to form a microscopic airtight "balloon",[27] which clearly demonstrates its property as an

*Address correspondence to r.ruoff@mail.utexas.edu, jpark@cornell.edu.

Received for review November 8, 2010 and accepted January 13, 2011.

Published online January 28, 2011
10.1021/nn103028d

impermeable barrier. Second, graphene has exceptional thermal and chemical stability. Under an inert environment it is stable at extremely high temperatures (higher than 1500 °C[28−30]) and it is also stable under many conditions where other substrates would undergo rapid chemical reactions. In fact, the latter property has been the key to the processes used to separate large scale graphene from the substrates where they are grown. Combined, these two properties (impermeability and thermal/chemical stability) alone would make graphene an excellent candidate for a novel protection layer. Furthermore, graphene has several unique benefits. It is optically transparent (approximately 2.3% absorption per layer[31]) in visible wavelengths, electrically and thermally conductive, and it adds only about 0.34 nm per layer to the total dimension of the coated metal. To the best of our knowledge, the use of graphene as a passivation layer to protect metal surfaces has not been reported yet.

In this work, we demonstrate for the first time the ability of graphene films grown by CVD to protect the surface of the metallic growth substrate (Cu and Cu/Ni alloys) from oxidation, both in air at elevated temperatures, as well as in hydrogen peroxide. Large area graphene was grown directly on Cu foils, and Cu/Ni alloys using methane as a carbon source by CVD. Details are discussed in the Methods section. The performance of the graphene coating as a transparent, conductive, and potentially passivating film on these metal foils was evaluated by heating the graphene-coated foils in an oven for 4 h at 200 °C in laboratory air, as well as immersing 1 cm^2 pieces of such graphene-coated metal foils into a solution of 30% (weight/weight) hydrogen peroxide (H_2O_2, Fisher Scientific) up to 45 min. Two types of samples were prepared: graphene-coated Cu foil (designated as Cu+G), and graphene-coated Cu/Ni alloy foil (designated as Cu/Ni+G). These samples were compared to corresponding untreated metal foils (designated as Cu and Cu/Ni).

RESULTS AND DISCUSSION

Prior to any studies, micro-Raman spectroscopy was performed on each sample in order to verify the presence of high quality graphene films. Single layer graphene films display sharp G (~1580 cm^{-1}) and 2D (~2700 cm^{-1}) bands, with a low G/2D ratio (typically smaller than 0.5).[16,17] Multilayer graphene can be identified by a high G/2D ratio (larger than or close to 1) and the altered shape of the 2D band.[32,33] Defect density is indicated by the D (~1350 cm^{-1})/G ratio,[34] which is negligible for pristine single crystal graphene.[35]

In Figure 1 we show photograph images of various metal surfaces, both graphene-coated and uncoated, after air anneals and exposure to liquid etchant. In all cases the graphene-coated metal surfaces show very little visible change, as opposed to the uncoated metals whose surfaces change appearance dramatically. As

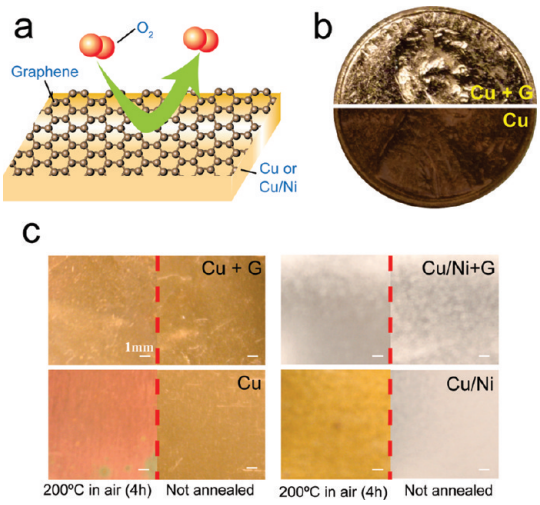

Figure 1. (a) Illustration depicting a graphene sheet as a chemically inert diffusion barrier. (b) Photograph showing graphene coated (upper) and uncoated (lower) penny after H_2O_2 treatment (30%, 2 min). (c) Photographs of Cu and Cu/Ni foil with and without graphene coating taken before and after annealing in air (200 °C, 4 h).

schematically shown in Figure 1a, the graphene film can be seen as a molecular diffusion barrier, preventing the reactive agent from ever reaching the metal underneath. More specifically, graphene-coated Cu and Cu/Ni foils show no changes after lengthy air anneals (200 °C, 4 h, see Figure 1c), whereas uncoated films exhibited a substantial darkening. To further demonstrate the potential of graphene as a protection layer for bulk metal, we grew single layer graphene on a copper penny (95%Cu/5% Zn, minted 1962−1982). In Figure 1b two penny halves are displayed, both of which were exposed to 30% H_2O_2 for 2 min. Although both pennies originally looked the same, a stark contrast arises between the graphene-coated (upper) and uncoated (lower) coins after exposure. The unprotected copper penny turned a dark shade of brown, whereas the protected coin maintained the original appearance. All these examples show that graphene passivates the growth surface, which, as discussed earlier, is due to its impermeability and chemical resistance. Below we discuss these two aspects in more detail.

Figure 2 shows SEM and XPS measurements of metal surfaces before and after air oxidation. The atomic steps under the graphene film are clearly visible for graphene-coated samples before and after the anneals (Figure 2a,c, top), indicating that copper oxide has not formed beneath the graphene. The coated Cu and Cu/Ni surface is free from surface oxide due to the H_2(g) exposure at a high temperature (1000 °C) prior to the growth of graphene. The metal surface is protected by the graphene layer during subsequent extended exposure at 200 °C in air. The micrograph has a number of small bright white spots representing oxides formed, most likely at the graphene grain boundaries or defect

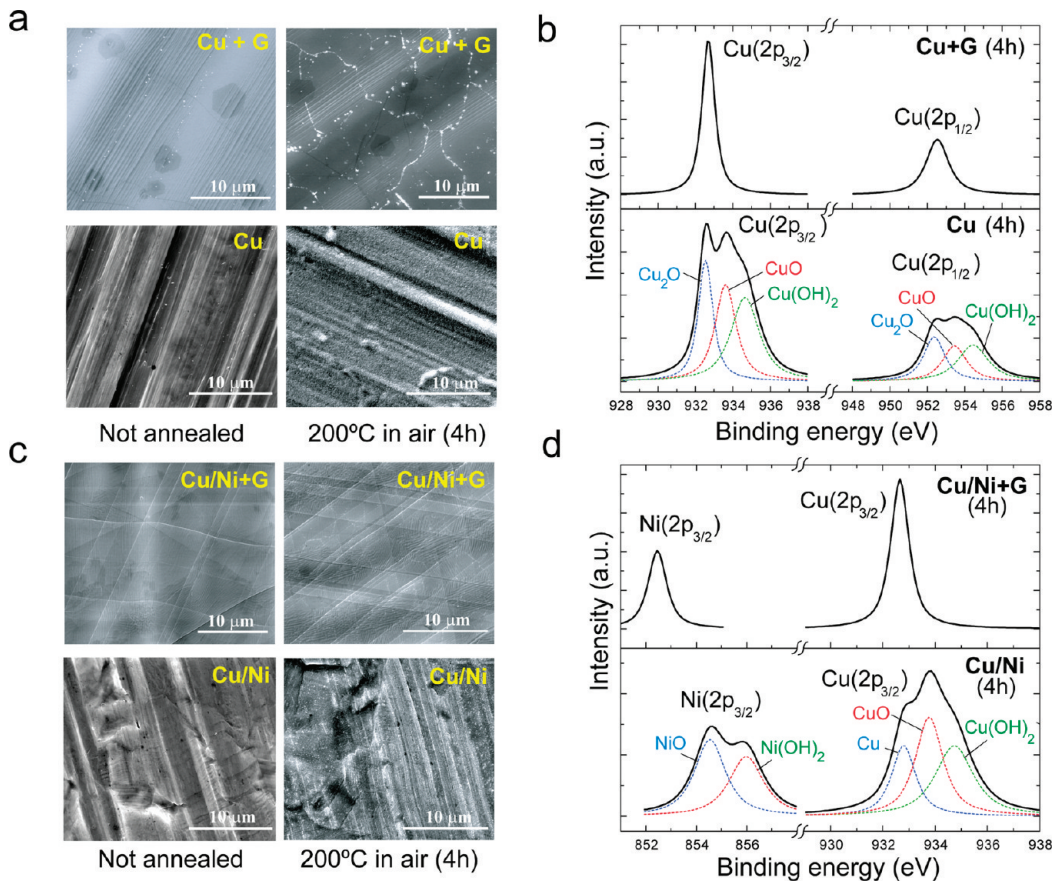

Figure 2. (a) SEM images of graphene coated (upper) and uncoated (lower) Cu foil taken before (left column) and after (right column) annealing in air. (b) XPS core-level Cu2p spectrum of coated (upper) and uncoated (lower) Cu foil after air anneal (200 °C, 4 h). (c) SEM images of graphene coated (upper) and uncoated (lower) Cu/Ni foil taken before (left column) and after (right column) annealing in air. (d) XPS core-level $Ni2p_{3/2}$ and $Cu2p_{3/2}$ spectrum of coated (upper) and uncoated (lower) Cu/Ni foil after air anneal (200 °C, 4 h).

sites of the graphene surface, as we presented in a previous paper.[18] Better protection is afforded for the Cu/Ni alloy foil surface by a multilayer (as confirmed by the measured Raman ratio of the G/2D band in Figure 3 for Cu/Ni+G (0 h)) graphene coating. In contrast, images of unprotected metal foils after annealing show a rough surface structure and are much more blurry—likely due to a charging effect from the presence of oxides. It is difficult to obtain a clear image because of the accumulated charges in insulating oxides on the surface.

XPS was then performed on these substrates in order to provide an analysis of the metal composition after heat treatment (200 °C, 4 h). The XPS spectra of coated Cu foil before and after air annealing (200 °C, 4 h) both show two Cu peaks at binding energies of 932.6 and 952.5 eV, which correspond to $Cu2p_{3/2}$ and $Cu2p_{1/2}$ (Figure 2b).[36,37] However, uncoated Cu foil shows broader peaks which correspond to different copper oxides, Cu_2O (932.5 and 952.3 eV), CuO (933.6 and 953.4 eV), and $Cu(OH)_2$ (934.7 and 954.5 eV).[36,37] These data indicate that the graphene coating is clearly acting as a diffusion barrier, protecting the underlying copper from oxidation. Similarly, Figure 2d shows the XPS spectrum for the coated Cu/Ni foil. Two sharp peaks are present, corresponding to $Cu2p_{3/2}$ (932.6 eV) and $Ni2p_{3/2}$ (852.5 eV),[36] demonstrating no change in the chemical composition of the protected metal. As before, inspection of the uncoated foil reveals two broader peaks, one is composed of two nickel oxide peaks, NiO (854.5 eV) and $Ni(OH)_2$ (856.0 eV),[36,38] and the other is composed of three peaks—metallic Cu (932.6 eV) and two copper oxide peaks, CuO (933.6 eV), and $Cu(OH)_2$ (934.7 eV). These XPS spectra demonstrate that the uncoated Cu/Ni foil was oxidized to a certain extent after heat treatment. The data in Figure 2d also provide a means to compare graphene as a protection layer with the Cu/Ni alloy inherent corrosion resistance. Upon oxidation the uncoated Cu/Ni alloy forms a protective film of Cu_2O with Ni compounds (*e.g.*, NiO) as minor components.[39,40] This oxide layer is more stable due to the presence of Ni atoms in the copper lattice, resulting in a lower number of defects.[39,41] The oxide therefore provides better protection against further oxidation, which explains the presence of a metallic Cu signal in Figure 2d (lower). Nevertheless, in our experiments the graphene-coated Cu/Ni alloy still shows significantly better oxidation

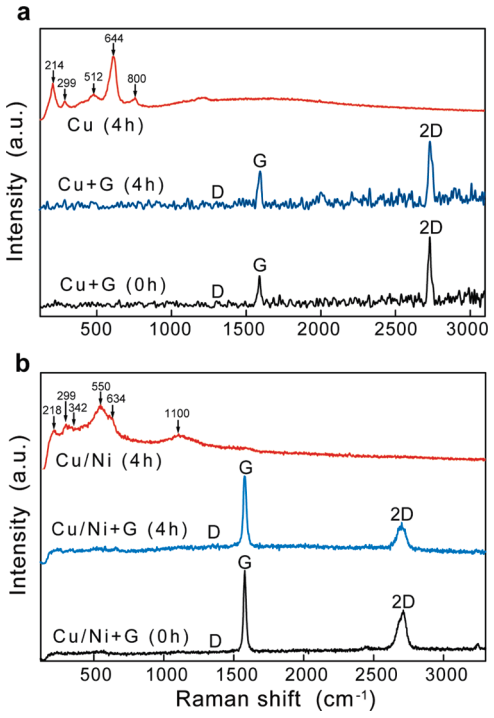

Figure 3. Raman spectrum of the Cu (a) and Cu/Ni alloy (b) foils with and without a graphene coating, acquired following heating in air at 200 °C for 0 and 4 h, respectively.

resistance, compared to the uncoated Cu/Ni alloy, as can be seen from the absence of oxide signals in Figure 2d (upper).

Under air oxidation graphene also shows remarkable chemical stability. Figure 3 presents the Raman spectra of coated and uncoated Cu and Cu/Ni foil samples, before and after heating in air (200 °C, 4 h). Before treatment, the coated Cu foil exhibits a small G/2D peak ratio ~0.5 which is indicative of high quality single layer graphene.[35] The coated Cu/Ni foil also exhibits characteristics of high quality multilayer graphene—a low D band in conjunction with the distinct G and 2D peak shapes. After heat treatment, the uncoated Cu foil shows multiple peaks between 214 and 800 cm^{-1}, corresponding to various copper oxides—Cu_2O (214, 644 cm^{-1}), CuO (299, 500 cm^{-1}), and Cu $(OH)_2$ (800 cm^{-1}).[42,43] Uncoated Cu/Ni foil displays CuO (299, 342, 634 cm^{-1}) and Cu_2O (218 cm^{-1}) peaks as well as NiO peaks (550 and 1100 cm^{-1}).[44,45] In contrast, the initial and final spectra of the coated foils are essentially identical. This clearly shows that the graphene is not only protecting the underlying metal but is also virtually unaltered by the oxidizing gas. The data shown in Figures 2 and 3 illustrate that both single layer and multilayer graphene serve as ideal protection coatings by both preventing diffusion and remaining chemically inert. Surprisingly, this oxidation protection by graphene is possible without strong adhesion to metal surfaces. Theory done to date indicates the interaction between graphene and the underneath metal is rather weak.[46–49] The graphene on Cu is considered to be physisorbed with a binding energy of $\Delta E < 0.07$ eV per carbon atom.[46]

To test longer term exposure, a run with 2 days exposure to air at 200 °C was performed on the graphene-coated Cu and Cu/Ni alloy samples. The Cu foils coated with monolayer graphene were oxidized to some extent, but a multilayer graphene-coated Cu/Ni foil remains visibly "shiny". The Raman spectrum obtained within graphene grains is identical to the 4 h anneal, with sharp G and 2D Raman bands. However, regions of oxidized metal surface that were formed along the grain boundaries of the graphene can be seen by SEM, suggesting that the grain boundary is more susceptible to oxidative reactions.

Short time exposure to the oxidizing aqueous solution of H_2O_2 showed also significant protection for both graphene-coated Cu and Cu/Ni alloy foils. Graphene-coated Cu and Cu/Ni samples were only attacked in few spots (white regions) after 15 and 5 min of H_2O_2 exposure, respectively (Figure 4). Once the metal is exposed, the liquid can easily penetrate underneath the graphene sheet to attack the metal, since there is no oxide layer to slow the corrosion. Examples of this are seen in both the graphene coated Cu and Cu/Ni samples after longer H_2O_2 exposure, 45 and 15 min, respectively. The slower etch rate of graphene-coated Cu than that of Cu/Ni might be due to the less reactive property of Cu than that of Ni in H_2O_2. The majority of the metal surface remains covered and protected by graphene.

In principle, "perfect" graphene, without defects and grain boundaries, is able to preserve the surface of metal under reactive environments over a long period of time thanks to its impermeability and chemical inertness. However, real CVD graphene is expected to show nonideal behaviors. It is known that graphene is more likely to react at edges or where defects are present such as wrinkles and point defect as well as graphene boundaries.[50] Our results in Figure 2a suggest that grain boundaries are likely to be the main contributor to oxidation of the underlying metals. The molecular diffusion through graphene grain boundaries, a crucial factor for understanding effective oxidation protection, would be affected by many factors, mainly the structure and chemical activity of grain boundaries and the surface oxidation rates. *In-situ* imaging techniques, such as LEEM[51] and TEM[52] are only starting to emerge and would be a powerful tool for future characterization of oxidation along grain boundaries.

One way to address oxidation through grain boundaries is to grow high quality and large domain single crystal graphene. Strong interest in nanoelectronics and other applications such as thermal management has already driven many groups around the world, our group included, to engineer grain structures and boundaries, and to rapidly increase graphene grain size. For example, we have recently achieved near

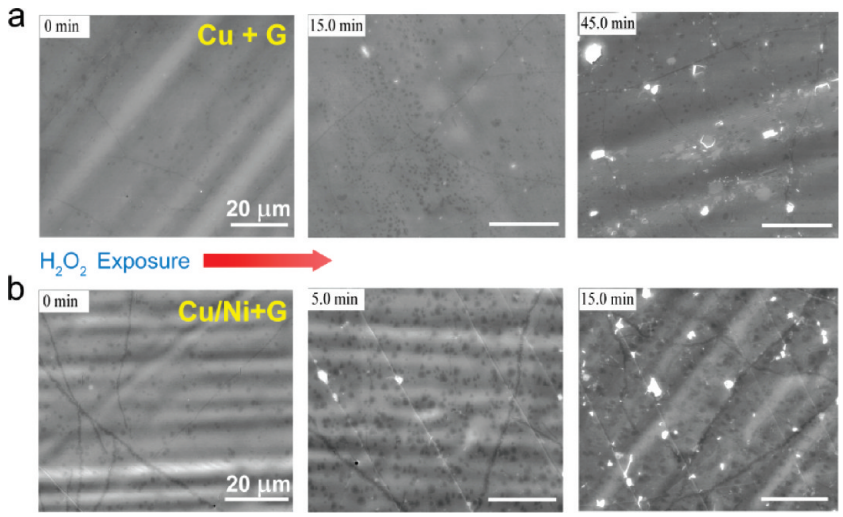

Figure 4. (a) SEM images of graphene-coated Cu film after 30% H_2O_2 exposure for (left) 0, (middle) 15, and (right) 45 min. (b) SEM images of graphene coated Cu/Ni alloy after 30% H_2O_2 exposure for (left) 0, (middle) 5, and (right) 15 min.

millimeter-sized grains in CVD growth of monolayer graphene on Cu.[53] Another way is to extend study to ultrathin graphite or hexagonal boron nitride thin films. The protection technique discussed here should work on any metals that can effectively catalyze graphene or ultrathin graphite growth, for example, Cu, Ni, Fe, Ta, Pt, Ir, Ru, and their alloys. Furthermore, refinement of graphene (multilayer graphene, ultrathin graphite) transfer techniques may allow their broader use on arbitrary substrates.

Further work is underway to explore graphene's functionality as an anticorrosion protective coating for nanoelectronic devices and other applications. This discovery would lead the worldwide graphene synthesis community to implement these novel applications of graphene, multilayer graphene, and ultrathin graphite as passivation coatings. The main limitation of this protection technique is its deactivation after mechanical damage. Therefore we would suggest using this protective coating on applications that do not involve circumstances where abrasion would ever be present, such as replacement of the Au coating for passivating Cu lines in semiconductor chip technology.

CONCLUSIONS

We demonstrate for the first time the excellent performance of graphene as a passivation layer. The ability of graphene coating to both prevent diffusion, as well as its chemical inertness to oxidizing gas and liquid solutions allow for its use in a wide variety of environments. Although partial oxidation may occur at graphene grain boundaries, we note that the graphene sheets provide near perfect protection within grains. With further advances in graphene growth and careful control of the metal catalyst, we anticipate a significant improvement in the level of protection these films may provide. Furthermore, refinement of graphene transfer techniques may even make it possible to take advantage of this material's amazing properties in any compatible system.

METHODS

Preparation. Large-area graphene samples were grown on metal substrates using previously reported CVD techniques.[17,19] Growth of graphene on Cu foil (99.8% Alfa Aesar no. 13382) was performed in a hot wall tube furnace at a temperature of 1040 °C with 5% H_2 (ultra high purity; grade Air Gas, Inc.) in CH_4 (ultra high purity; grade Air Gas, Inc.) at a pressure of 500 mTorr. Growth of graphene on Cu/Ni (31% Ni, 67.8% Cu, 0.45% Mn, 0.60% Fe, else 0.15%, All Metal Sales, Inc.) was performed in the cold-wall CVD system at a growth temperature of 1000 °C with pure CH_4 at a pressure of 8 Torr.

Characterization. SEM images were taken with an FEI Quanta-600 FEG Environmental SEM using a voltage of 30 KV. XPS data were acquired to determine the chemical composition of the graphene films using a Kratos AXIS Ultra DLD XPS equipped with a 1808 hemispherical energy analyzer with photoemission stimulated by a monochromated Al Ka radiation source (1486.6 eV) at an operating power of 150 W. It was operated in the analyzer mode at 80 eV for survey scans and 20 eV for detailed scans of core level lines. Binding energies were referenced to the C 1s binding energy set at 284.5 eV. Curve fitting of each spectrum was performed using a Gaussian–Lorentzian peak shape after performing a Shirley background correction using Kratos Vision v2.2 software. Raman spectra (WITec Alpha 300) were obtained with a 532 nm laser (~50 mW power).

Acknowledgment. This work was supported by the Office of Naval Research and the DARPA Carbon Electronics for RF Applications Center, Center for Molecular Interfacing and Cornell Center for Materials Research, both funded by NSF, AFOSR PECASE, and IO. S. Chen and J. Kang are supported by the CSC Fellowship, "973" Program (2011CB925600), and the National Natural Science Foundation (Grants 60827004 and 90921002) of

China. L.B. is partially supported by a Fulbright fellowship. M.L is supported by an NSF IGERT training fellowship.

REFERENCES AND NOTES

1. Gray, J. E.; Luan, B. Protective Coatings on Magnesium and Its Alloys—A Critical Review. *J. Alloys Compd.* **2002,** *336*, 88–113.
2. Rao, B. V. A.; Iqbal, M. Y.; Sreedhar, B. Self-Assembled Monolayer of 2-(Octadecylthio)benzothiazole for Corrosion Protection of Copper. *Corros. Sci.* **2009,** *51*, 1441–1452.
3. Stratmann, M.; Feser, R.; Leng, A. Corrosion Protection by Organic Films. *Electrochim. Acta* **1994,** *39*, 1207–1214.
4. Merkula, D. M.; Novikov, P. D.; Ivanenkov, V. N.; Sapozhnikov, V. V.; Lyakhin, Y. I. Utilization of EDN Varnish for Protection of Metal Sea-Water Sampling Bottles Against Corrosion. *Oceanol., USSR* **1974,** *14*, 299–300.
5. Redondo, M. I.; Breslin, C. B. Polypyrrole Electrodeposited on Copper from an Aqueous Phosphate Solution: Corrosion Protection Properties. *Corros. Sci.* **2007,** *49*, 1765–1776.
6. Mittal, V. K.; Bera, S.; Saravanan, T.; Sumathi, S.; Krishnan, R.; Rangarajan, S.; Velmurugan, S.; Narasimhan, S. V. Formation and Characterization of Bilayer Oxide Coating on Carbon-Steel for Improving Corrosion Resistance. *Thin Solid Films* **2009,** *517*, 1672–1676.
7. Kinlen, P. J.; Menon, V.; Ding, Y. W. A Mechanistic Investigation of Polyaniline Corrosion Protection Using the Scanning Reference Electrode Technique. *J. Electrochem. Soc.* **1999,** *146*, 3690–3695.
8. Grundmeier, G.; Reinartz, C.; Rohwerder, M.; Stratmann, M. Corrosion Properties of Chemically Modified Metal Surfaces. *Electrochim. Acta* **1998,** *43*, 165–174.
9. Segarra, M.; Miralles, L.; Diaz, J.; Xuriguera, H.; Chimenos, J. M.; Espiell, F.; Pinol, S. Copper and CuNi Alloys Substrates for HTS Coated Conductor Applications Protected from Oxidation. *Mater. Sci. Forum* **2003,** *426−4*, 3511–3516.
10. Novoselov, K. S.; Geim, A. K.; Morozov, S. V.; Jiang, D.; Katsnelson, M. I.; Grigorieva, I. V.; Dubonos, S. V.; Firsov, A. A. Two-Dimensional Gas of Massless Dirac Fermions in Graphene. *Nature* **2005,** *438*, 197–200.
11. Novoselov, K. S.; Geim, A. K.; Morozov, S. V.; Jiang, D.; Zhang, Y.; Dubonos, S. V.; Grigorieva, I. V.; Firsov, A. A. Electric Field Effect in Atomically Thin Carbon Films. *Science* **2004,** *306*, 666–669.
12. Zhang, Y. B.; Tan, Y. W.; Stormer, H. L.; Kim, P. Experimental Observation of the Quantum Hall Effect and Berry's Phase in Graphene. *Nature* **2005,** *438*, 201–204.
13. Lu, X. K.; Yu, M. F.; Huang, H.; Ruoff, R. S. Tailoring Graphite with the Goal of Achieving Single Sheets. *Nanotechnology* **1999,** *10*, 269–272.
14. Yu, Q. K.; Lian, J.; Siriponglert, S.; Li, H.; Chen, Y. P.; Pei, S. S. Graphene Segregated on Ni Surfaces and Transferred to Insulators. *Appl. Phys. Lett.* **2008,** *93*, 113103.
15. Kim, K. S.; Zhao, Y.; Jang, H.; Lee, S. Y.; Kim, J. M.; Ahn, J. H.; Kim, P.; Choi, J. Y.; Hong, B. H. Large-Scale Pattern Growth of Graphene Films for Stretchable Transparent Electrodes. *Nature* **2009,** *457*, 706–710.
16. Reina, A.; Jia, X. T.; Ho, J.; Nezich, D.; Son, H. B.; Bulovic, V.; Dresselhaus, M. S.; Kong, J. Large Area, Few-Layer Graphene Films on Arbitrary Substrates by Chemical Vapor Deposition. *Nano Lett.* **2009,** *9*, 30–35.
17. Li, X. S.; Cai, W. W.; An, J. H.; Kim, S.; Nah, J.; Yang, D. X.; Piner, R.; Velamakanni, A.; Jung, I.; Tutuc, E.; *et al.* Large-Area Synthesis of High-Quality and Uniform Graphene Films on Copper Foils. *Science* **2009,** *324*, 1312–1314.
18. Li, X. S.; Cai, W. W.; Colombo, L.; Ruoff, R. S. Evolution of Graphene Growth on Ni and Cu by Carbon Isotope Labeling. *Nano Lett.* **2009,** *9*, 4268–4272.
19. Li, X. S.; Cai, W. W.; Jung, I. H.; An, J. H.; Yang, D. X.; Velamakanni, A.; Piner, R.; Colombo, L.; Ruoff, R. S. Synthesis, Characterization, and Properties of Large-Area Graphene Films. *ECS Trans.* **2009,** *19*, 41–52.
20. Fujita, T.; Kobayashi, W.; Oshima, C. Novel Structures of Carbon Layers on a Pt(111) Surface. *Surf. Interface Anal.* **2005,** *37*, 120–123.
21. Coraux, J.; N'Diaye, A. T.; Busse, C.; Michely, T. Structural Coherency of Graphene on Ir(111). *Nano Lett.* **2008,** *8*, 565–570.
22. Cai, W. W.; Zhu, Y. W.; Li, X. S.; Piner, R. D.; Ruoff, R. S. Large Area Few-Layer Graphene/Graphite Films as Transparent Thin Conducting Electrodes. *Appl. Phys. Lett.* **2009,** *95*, 123115.
23. Sutter, P. W.; Flege, J. I.; Sutter, E. A. Epitaxial Graphene on Ruthenium. *Nat. Mater.* **2008,** *7*, 406–411.
24. Kondo, D.; Sato, S.; Yagi, K.; Harada, N.; Sato, M.; Nihei, M.; Yokoyama, N. Low-Temperature Synthesis of Graphene and Fabrication of Top-Gated Field Effect Transistors without Using Transfer Processes. *Appl. Phys. Express* **2010,** *3*, 025102.
25. Kumar, S.; McEvoy, N.; Lutz, T.; Keeley, G. P.; Whiteside, N.; Blau, W.; Duesberg, G. S. Low Temperature Graphene Growth. *ECS Trans.* **2009,** *19*, 175–181.
26. Holt, J. K.; Park, H. G.; Wang, Y. M.; Stadermann, M.; Artyukhin, A. B.; Grigoropoulos, C. P.; Noy, A.; Bakajin, O. Fast Mass Transport Through Sub-2-nanometer Carbon Nanotubes. *Science* **2006,** *312*, 1034–1037.
27. Bunch, J. S.; Verbridge, S. S.; Alden, J. S.; van der Zande, A. M.; Parpia, J. M.; Craighead, H. G.; McEuen, P. L. Impermeable Atomic Membranes from Graphene Sheets. *Nano Lett.* **2008,** *8*, 2458–2462.
28. de Heer, W. A.; Berger, C.; Wu, X. S.; First, P. N.; Conrad, E. H.; Li, X. B.; Li, T. B.; Sprinkle, M.; Hass, J.; Sadowski, M. L.; *et al.* Epitaxial Graphene. *Solid State Commun.* **2007,** *143*, 92–100.
29. Hass, J.; Varchon, F.; Millan-Otoya, J. E.; Sprinkle, M.; Sharma, N.; De Heer, W. A.; Berger, C.; First, P. N.; Magaud, L.; Conrad, E. H. Why Multilayer Graphene on 4H-SiC(000$\bar{1}$) Behaves Like a Single Sheet of Graphene. *Phys. Rev. Lett.* **2008,** *100*, 125504.
30. Shivaraman, S.; Chandrashekhar, M. V. S.; Boeckl, J. J.; Spencer, M. G. Thickness Estimation of Epitaxial Graphene on SiC Using Attenuation of Substrate Raman Intensity. *J. Electron. Mater.* **2009,** *38*, 725–730.
31. Nair, R. R.; Blake, P.; Grigorenko, A. N.; Novoselov, K. S.; Booth, T. J.; Stauber, T.; Peres, N. M. R.; Geim, A. K. Fine Structure Constant Defines Visual Transparency of Graphene. *Science* **2008,** *320*, 1308–1308.
32. Reina, A.; Son, H. B.; Jiao, L. Y.; Fan, B.; Dresselhaus, M. S.; Liu, Z. F.; Kong, J. Transferring and Identification of Single- and Few-Layer Graphene on Arbitrary Substrates. *J. Phys. Chem. C* **2008,** *112*, 17741–17744.
33. Malard, L. M.; Pimenta, M. A.; Dresselhaus, G.; Dresselhaus, M. S. Raman Spectroscopy in Graphene. *Phys. Rep.* **2009,** *473*, 51–87.
34. Tuinstra, F.; Koenig, J. L. Raman Spectrum of Graphite. *J. Chem. Phys.* **1970,** *53*, 1126–1130.
35. Ferrari, A. C.; Meyer, J. C.; Scardaci, V.; Casiraghi, C.; Lazzeri, M.; Mauri, F.; Piscanec, S.; Jiang, D.; Novoselov, K. S.; Roth, S.; Geim, A. K. Raman Spectrum of Graphene and Graphene Layers. *Phys. Rev. Lett.* **2006,** *97*, 187401.
36. Dube, C. E.; Workie, B.; Kounaves, S. P.; Robbat, A.; Aksu, M. L.; Davies, G. Electrodeposition of Metal Alloy and Mixed-Oxide Films Using a Single-Precursor Tetranuclear Copper-Nickel Complex. *J. Electrochem. Soc.* **1995,** *142*, 3357–3365.
37. Poulston, S.; Parlett, P. M.; Stone, P.; Bowker, M. Surface Oxidation and Reduction of CuO and Cu_2O Studied Using XPS and XAES. *Surf. Interface Anal.* **1996,** *24*, 811–820.
38. Sasi, B.; Gopchandran, K. G. Nanostructured Mesoporous Nickel Oxide Thin Films. *Nanotechnology* **2007,** *18*, 115613.
39. Yuan, S. J.; Pehkonen, S. O. Surface Characterization and Corrosion Behavior of 70/30 Cu-Ni Alloy in Pristine and Sulfide-Containing Simulated Seawater. *Corros. Sci.* **2007,** *49*, 1276–1304.
40. Kato, C.; Castle, J. E.; Ateya, B. G.; Pickering, H. W. On the Mechanism of Corrosion of $Cu_{9.4}Ni_{1.7}Fe$ Alloy in Air Saturated

Aqueous NaCl Solution. *J. Electrochem. Soc.* **1980,** *127*, 1987–2003.
41. Druska, P.; Strehblow, H. H.; Golledge, S. A Surface Analytical Examination of Passive Layers on Cu/Ni Alloys: Part I. Alkaline Solution. *Corros. Sci.* **1996,** *38*, 835–851.
42. Niaura, G. Surface-Enhanced Raman Spectroscopic Observation of Two Kinds of Adsorbed OH-Ions at Copper Electrode. *Electrochim. Acta* **2000,** *45*, 3507–3519.
43. Chou, M. H.; Liu, S. B.; Huang, C. Y.; Wu, S. Y.; Cheng, C. L. Confocal Raman Spectroscopic Mapping Studies on a Single CuO Nanowire. *Appl. Surf. Sci.* **2008,** *254*, 7539–7543.
44. Ishida, Y.; Mita, Y.; Kobayashi, M.; Endo, S. Pressure Effects on Transition Metal Monoxide NiO. *Phys. Status Solidi B* **2003,** *235*, 501–504.
45. Mendoza, L.; Baddour-Hadjean, R.; Cassir, M.; Pereira-Ramos, J. P. Raman Evidence of the Formation of LT-$LiCoO_2$ Thin Layers on NiO in Molten Carbonate at 650 °C. *Appl. Surf. Sci.* **2004,** *225*, 356–361.
46. Giovannetti, G.; Khomyakov, P. A.; Brocks, G.; Karpan, V. M.; van den Brink, J.; Kelly, P. J. Doping Graphene with Metal Contacts. *Phys. Rev. Lett.* **2008,** *101*, 026803.
47. Qi, Y.; Hector, L. G.; Ooi, N.; Adams, J. B. A First Principles Study of Adhesion and Adhesive Transfer at Al(111)/graphite(0001). *Surf. Sci.* **2005,** *581*, 155–168.
48. Gamo, Y.; Nagashima, A.; Wakabayashi, M.; Terai, M.; Oshima, C. Atomic Structure of Monolayer Graphite Formed on Ni(111). *Surf. Sci.* **1997,** *374*, 61–64.
49. Bertoni, G.; Calmels, L.; Altibelli, A.; Scrin, V. First-Principles Calculation of the Electronic Structure and EELS Spectra at the Graphene/Ni(III) Interface. *Phys. Rev. B* **2005,** *71*, 075402.
50. Jiang, D. E.; Sumpter, B. G.; Dai, S. Unique Chemical Reactivity of a Graphene Nanoribbon's Zigzag Edge. *J. Chem. Phys.* **2007,** *126*, 134701.
51. Wofford, J. M.; Nie, S.; McCarty, K. F.; Bartelt, N. C.; Dubon, O. D. Graphene Islands on Cu Foils: The Interplay between Shape, Orientation, and Defects. *Nano Lett.* **2010,** *10*, 4890–4896.
52. Huang, P. Y.; Ruiz-Vargas, C. S.; Van der Zande, A. M.; Whitney, W. S.; Levendorf, M. P.; Kevek, J. W.; Garg, S.; Alden, J. S.; Hustedt., C. J.; Zhu, Y. Grains and Grain Boundaries in Single-Layer Graphene Atomic Patchwork Quilts. *Nature* **2011**, *469*, 389−392.
53. Li, X. S.; Magnuson, C. W.; Venugopal, A.; Tromp, R. M.; Hannon, J. B.; Colombo, L.; Ruoff, R. S., Large Area Graphene Single Crystals Grown by Low Pressure Chemical Vapor Deposition of Methane on Copper. *J. Am. Chem. Soc.* Submitted for publication.